SATELLITE FORMATION DESIGN FOR SPACE BASED RADAR APPLICATIONS

Dr. Steven Tragesser

Department of Mechanical and Aerospace Engineering
University of Colorado at Colorado Springs
1420 Austin Bluffs Parkway
P.O. Box 7150
Colorado Springs, CO 80933-7150

30 July 2007

Final Report

AIR FORCE RESEARCH LABORATORY
Space Vehicles Directorate
3550 Aberdeen Ave SE
AIR FORCE MATERIEL COMMAND
KIRTLAND AIR FORCE BASE, NM 87117-5776

NOTICE AND SIGNATURE PAGE

Using Government drawings, specifications, or other data included in this document for any purpose other than Government procurement does not in any way obligate the U.S. Government. The fact that the Government formulated or supplied the drawings, specifications, or other data does not license the holder or any other person or corporation; or convey any rights or permission to manufacture, use, or sell any patented invention that may relate to them.

This report was cleared for public release by the Air Force Research Laboratory/KAFB Public Affairs Office and is available to the general public, including foreign nationals. Copies may be obtained from the Defense Technical Information Center (DTIC) (http://www.dtic.mil).

AFRL-RV-PS-TR-2007-1141 HAS BEEN REVIEWED AND IS APPROVED FOR PUBLICATION IN ACCORDANCE WITH ASSIGNED DISTRIBUTION STATEMENT.

//signed//	//signed//
THOMAS ALAN LOVELL, DR-II Program Manager	WADE H. VAUGHT, LT COL, USAF Acting Chief, Integrated Experiments & Evaluation Division

This report is published in the interest of scientific and technical information exchange, and its publication does not constitute the Government's approval or disapproval of its ideas or findings.

REPORT DOCUMENTATION PAGE

Form Approved
OMB No. 0704-0188

1. REPORT DATE *(DD-MM-YYYY)*	**2. REPORT TYPE**	**3. DATES COVERED** *(From - To)*
30 July 2007	Final	1 July 06 – 30 June 07

4. TITLE AND SUBTITLE

Satellite Formation Design for Space Based Radar Applications

5a. CONTRACT NUMBER
FA9453-06-M-0213

5b. GRANT NUMBER

5c. PROGRAM ELEMENT NUMBER
63401F

6. AUTHOR(S)
Dr. Steven Tragesser

5d. PROJECT NUMBER
2181

5e. TASK NUMBER
MA

5f. WORK UNIT NUMBER
AG

7. PERFORMING ORGANIZATION NAME(S) AND ADDRESS(ES)
Department of Mechanical and Aerospace Engineering
University of Colorado at Colorado Springs
1420 Austin Bluffs Parkway
P.O. Box 7150
Colorado Springs, CO 80933-7150

8. PERFORMING ORGANIZATION REPORT

9. SPONSORING / MONITORING AGENCY NAME(S) AND ADDRESS(ES)
Air Force Research Laboratory
Space Vehicles Directorate
3550 Aberdeen Ave SE
Kirtland AFB, NM 87117-5776

10. SPONSOR/MONITOR'S ACRONYM(S)
AFRL/RVES

11. SPONSOR/MONITOR'S REPORT NUMBER(S)
AFRL-RV-PS-TR-2007-1141

12. DISTRIBUTION / AVAILABILITY STATEMENT
Approved for public release; distribution is unlimited. (VS07-0691 dated 7 Dec 07)

13. SUPPLEMENTARY NOTES

14.ABSTRACT

There is much interest in relative formations in low Earth orbit for many different applications including distributed aperture systems and communications. Methods have been developed to create relative trajectories that do not fight the natural motion caused by oblateness perturbations. The formulas for these "J_2 Invariant" formations are recast in terms of relative orbit parameters that facilitate formation design. Impulsive maneuver schemes have also been developed for relative trajectories but they do not allow for multiple maneuvers for tight control. In this report, a process is developed to create relative orbits that meet design criteria while also not fighting natural motion. A maneuver scheme is employed that allows for tight control and several maneuvers per orbit. A Monte Carlo simulation is performed to assess the performance of this guidance approach with navigation and control errors.

15. SUBJECT TERMS
Astrodynamics; Modeling, Simulation, and Analysis; Satellite Formation Flying

16. SECURITY CLASSIFICATION OF:			**17. LIMITATION OF ABSTRACT**	**18. NUMBER OF PAGES**	**19a. NAME OF RESPONSIBLE PERSON**
					Dr. Thomas Alan Lovell
a. REPORT Unclassified	**b. ABSTRACT** Unclassified	**c. THIS PAGE** Unclassified	Unlimited	49	**19b. TELEPHONE NUMBER** *(include area code)* 505-853-4132

Standard Form 298 (Rev. 8-98)
Prescribed by ANSI Std. 239.18

Intentionally Left Blank

TABLE OF CONTENTS

LIST OF FIGURES

LIST OF TABLES

Intentionally Left Blank

CHAPTER 1. INTRODUCTION

There is much interest in relative formations in low Earth orbit for many different applications including distributed aperture systems and communications. While the Clohessy-Wiltshire Hills (CWH) equations have been in existence for sometime, it is more recently that they have been revisited to include perturbations in their formulation. Sabol, et al[1] developed a state transition matrix that included the secular effects of the oblateness of the Earth on relative trajectories. In Refs. 2 and 3, methods were developed so as to create relative orbits that were J_2 invariant. These works also developed the practice of using mean orbital elements to design relative orbits. Impulsive maneuver schemes have been developed in Refs. 3 and 4 that operate on differential orbital elements. A part of these approaches consists of a two burn sequence at periapsis and apoapsis. This limits the number of correction maneuvers to one per orbit. There are some similarities between Ref. 5 and this work, but the physical variables used in this report make it possible to formulate the nominal trajectory in terms of relative orbital elements that are more useful for design and analysis.

There are two major aims of this report. First is to develop a way of designing relative orbits that allows the designer to be able to specify aspects of the relative trajectory while trying to alleviate the effects of J_2 on the orbit. Second is to implement a maneuver scheme that allows for multiple corrections per orbit. Most of the work in this area to date does not allow for this and problems arise when tolerances on deviation are very low.

CHAPTER 2. RELATIVE FORMATIONS

For this paper, we are only concerned with the motion of a deputy satellite in relation to a chief satellite on a circular orbit. The position of the deputy is in respect to the chief in the Local Vertical-Local Horizontal (LVLH) frame. This frame of reference is fixed to the chief satellite. The x direction is along the zenith direction, y is in the alongtrack direction, and z is perpendicular to the orbital plane.

Using the parameterization from Ref. 6, the motion of the satellite is characterized according to the following equations:

$$\begin{aligned} x &= \frac{-a_e}{2}\cos\beta + x_d & \dot{x} &= \frac{a_e}{2} n \sin\beta \\ y &= a_e \sin\beta + y_d - \frac{3}{2} n x_d t & \dot{y} &= a_e n \cos\beta - \frac{3}{2} n x_d \\ z &= z_{\max} \sin(\gamma + \beta) & \dot{z} &= z_{\max} n \cos(\gamma + \beta) \end{aligned} \tag{1}$$

The equations above describe a relative ellipse that travels along the alongtrack direction. The relative orbital elements are as follows: a_e is the major axis of the ellipse, x_d and y_d describe offsets to the relative ellipse, in the zenith and alongtrack directions respectively, z_{max} is the maximum excursion out of the orbital plane, γ describes the orientation of the ellipse and

$$\beta = nt \tag{2}$$

These parameters are depicted in Fig. 1 for $x_d = y_d = 0$. The parameterized values for β and γ are related to the geometrical values in the figure, $\tilde{\beta}$ and $\tilde{\gamma}$, by:

$$\begin{aligned} \tan\tilde{\beta} &= 2\tan\beta \\ \tan\tilde{\gamma} &= 2\tan\gamma \end{aligned} \tag{3}$$

The projection of the path of the deputy satellite on to the x-y plane forms a 2x1 ellipse.

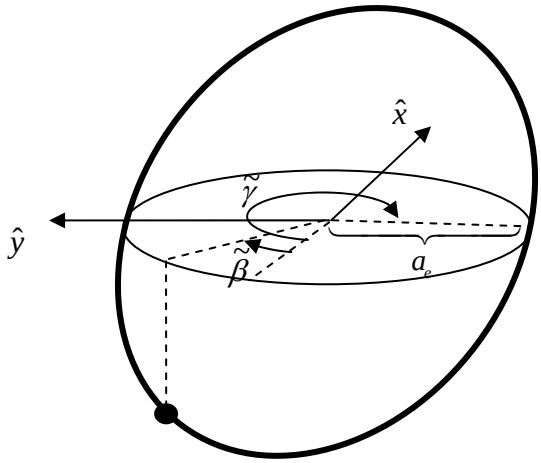

Figure 1: Relative Orbit

For unperturbed motion, a_e, x_d, y_d, z_{max}, and γ are all constant. The only time varying element is β. This gives a set of six elements that characterize a relative formation which will be referred to as the "relative orbital elements." For a closed formation, i.e. one in which all the satellites would remain in close proximity rather than drift apart, the secular term in the alongtrack equations must be eliminated by setting x_d=0. Setting x_d=0 is equivalent to constraining the orbit of the chief and the deputy to have the same semi major axis. In an unperturbed state this is also equivalent to setting the periods of the two satellites equal to each other. This is the only way to have a closed formation for unperturbed motion.

CHAPTER 3. OBLATENESS EFFECTS ON ORBITAL ELEMENTS

A. Definition of Orbital Elements

As defined in Ref. 7, there are six classical orbital elements which characterize the orbit. The first is the semi major axis, a, which relates the size of the orbit. Second is eccentricity, e, which determines the shape of the orbit, i.e. circular, elliptical, parabolic, or hyperbolic. For the purposes of this paper, we are only concerned with circular orbits which have an eccentricity of zero and elliptical orbits whose eccentricities are greater than zero and less than one. Third is the inclination, i, which relates the tilt of the orbit in relation to the equatorial plane. Fourth is the Right Ascension of the Ascending Node, Ω, which measures the angle between the line of Aries in the inertial frame and the point in the orbit where the satellite crosses from the south to the north hemisphere, also known as the ascending node. Fifth is the argument of perigee, ω, which measures the angle from the node to the point of closest approach to the Earth, or perigee. Last is the true anomaly, f, which measures the angle between perigee and the position of the satellite.

For this paper, several of these orbital elements are changed so as to avoid singularities and other complications. In a circular orbit, there is no perigee, so the angle used to determine the satellites current location is the true argument of latitude, θ, which is defined as $\theta=\omega+f$. Also in a circular orbit, the eccentricity is zero, which can cause singularities in several of the conversions to be used later in the paper. To overcome this, two new variables are introduced: q_1 and q_2. They are defined as[6]

$$q_1=e\cos\omega \text{ and } q_2=e\sin\omega \tag{4}$$

To determine the orbital elements of the deputy, the relative orbital elements are used with Eqs (1) to determine the relative state of the deputy in the LVLH frame. The chief's position and velocity in the inertial frame of reference are then transformed into a rotating frame of reference using Euler angle

rotations as laid out in Vallado[7]. The position of the deputy is found by adding the relative position vector to the rotating position vector of the chief. The velocity of the deputy in the rotating frame is found by adding the relative velocity and the velocity of the LVLH frame to that of the chief. The position and velocity of the deputy in the rotating frame are then transformed into the inertial frame through Euler angle rotations. The deputy orbital elements are then determined by using the deputy position and velocity following processes laid out in Ref. 7.

B. Equations of Motion

To numerically propagate an orbit, the equations of motion need to be developed. From Ref. 7, the basic two-body equation of motion is

$$\ddot{\bar{r}} = -\frac{\mu}{r^3}\bar{r} \tag{5}$$

Separating this equation into its components gives

$$\ddot{x} = -\frac{\mu}{r^3}x \quad \ddot{y} = -\frac{\mu}{r^3}y \quad \ddot{z} = -\frac{\mu}{r^3}z \tag{6}$$

This formulation is the unperturbed two-body equations of motion. To include the perturbations due to J_2, we take the partial derivatives of the disturbing function and add these effects to Eqs (6). Doing this yields the following equations of motion used to numerically propagate the satellite's orbit.

$$\begin{aligned}
\ddot{x} &= -\frac{\mu}{r^3}x - \frac{3J_2R_e^2x}{2r^5}\left(1-\frac{5z^2}{r^2}\right) \\
\ddot{y} &= -\frac{\mu}{r^3}y - \frac{3J_2R_e^2y}{2r^5}\left(1-\frac{5z^2}{r^2}\right) \\
\ddot{z} &= -\frac{\mu}{r^3}z - \frac{3J_2R_e^2z}{2r^5}\left(3-\frac{5z^2}{r^2}\right)
\end{aligned} \tag{7}$$

C. Oblateness Effects

When considering unperturbed two body motion, the only time varying orbital element is true anomaly. This is not the case when perturbations, especially the oblateness of the Earth, are included in the equations

of motion. When the oblateness of the Earth, specified by the J_2 term in the harmonic expansion in Ref. 7, is included, all of the orbital elements experience some periodic oscillations in their values. This is most easily seen in the values for semi major axis and inclination. An example case is illustrated using the following initial orbital elements for a satellite:

$$a= 7378 \text{ km}, \theta=0, i=50 \text{ deg}, q_1=0, q_2=0, \Omega=0 \text{ deg}$$

The orbit of the satellite is propagated using Eqs (7) and a numerical integration in MATLAB. Time histories of the semi major axis and inclination are shown in Figures 2 and 3, respectively, for a duration of 10 orbits. From these graphs, it is apparent that the mean values are not the initial values. The semi major axis average value is just under 7373 kilometers, from observation. Because of this difference between the initial values and the average value, we will define two different sets of orbital elements. The osculating orbital elements will be the instantaneous orbital elements at any point in time. The mean orbital elements will be the average orbital elements over time.

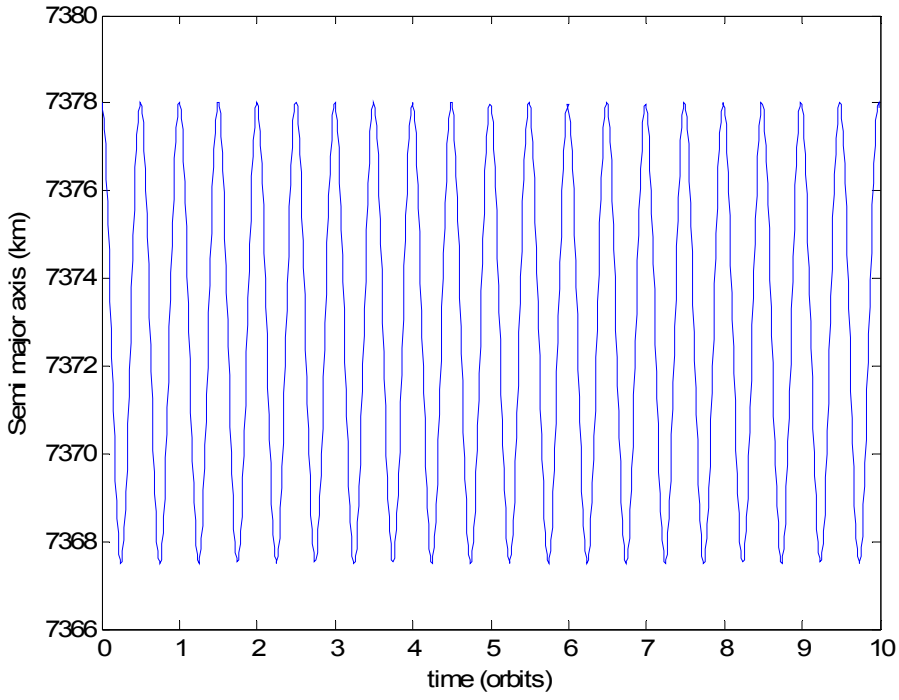

Figure 2: Time History of Semi Major Axis

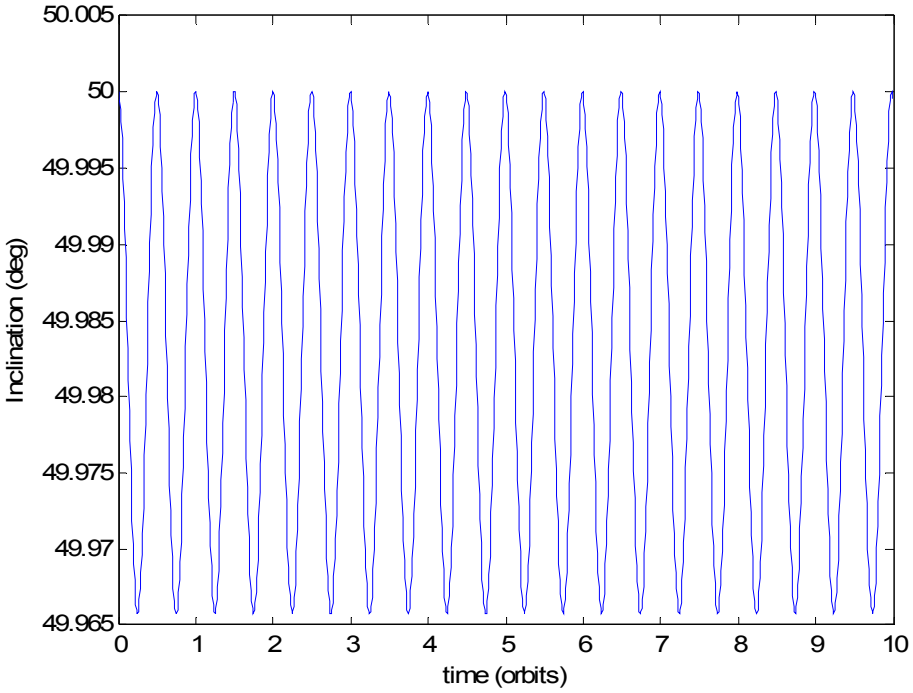

Figure 3: Time History of Inclination

D. Characterizing Perturbation Effects

To set up initial conditions that result in desired mean elements a conversion is used. To develop this conversion, the potential for J_2 gravity perturbation needs to be reformulated to show its effects on orbital elements. Following Kozai[8], the potential is

$$R(\bar{r}) = \frac{\mu J_2 R_e^2}{r^3}\left(-\frac{3}{2}\sin^2\phi + \frac{1}{2}\right) \tag{8}$$

where ϕ is the latitude of the sub-satellite point. Using relationships from spherical trigonometry, we are able to rearrange the equation into the form

$$R = \frac{\mu J_2 R_e^2}{2r^3}\left[1 - \frac{3}{2}\sin^2 i(1-\cos 2\theta)\right] \tag{9}$$

Kozai then breaks this disturbing potential into four parts: first and second order secular terms (linear in time), long period, and short period. To break out the first order secular effects, R_1, a Fourier series is used to isolate those terms. A relationship from Tisserand[9] is required and yields first order secular effects of

$$R_1 = \frac{\mu J_2 R_e^2}{2a^3}(1-\frac{3}{2}\sin^2 i)(1-e^2)^{-3/2} \tag{10}$$

As an example, to find the first order secular effects on RAAN, this equation is inserted into Lagrange's planetary equations to find

$$\dot{\Omega}_{\text{sec}} = \frac{1}{\bar{n}ab\sin i}\frac{\delta R_1}{\delta i} = -\frac{3\mu J_2 R_e^2}{2p^2 a^3 \bar{n}}\cos i \tag{11}$$

where $\bar{n}$ is the perturbed mean motion.

We also need to determine the short period effects on orbital elements. Using the potential equations, the short period effects are

$$R_4 = R - R_1 \tag{12}$$

Again, as an example, we will use the effect on RAAN. The disturbing potential is placed into the equation

$$\dot{\Omega}_{sp} = \frac{1}{na^2 \sin i}\frac{\delta R_4}{\delta i} \tag{13}$$

only retaining the terms to $\mathcal{O}(e)$. This equation needs to be integrated to determine the effects. First we need to change the variable of integration from time to true anomaly using the relationship

$$\delta t = \frac{1}{n}\left(\frac{r}{a}\right)^2 \frac{1}{\sqrt{1-e^2}}\delta f \tag{14}$$

Using this equation we are able to rearrange the terms to get

$$\Omega_{sp} = \int -\frac{3J_2 R_e^2 \cos i}{2a^2}\left[(1-\cos 2\theta)\left(\frac{a}{r}\right)-\left(\frac{r}{a}\right)^2\right]\delta f \tag{15}$$

Before we integrate we need to get this integral equation into terms of true anomaly. Using a Taylor series expansion and the formula

$$r = \frac{a(1-e^2)}{1+e\cos f} \tag{16}$$

along with several trigonometric identities we are able to get Eq (15) into a form suitable for integration. Integrating and rearranging the terms leads to the form

$$\Omega_{sp} = -\frac{3J_2R_e^2\cos i}{2a^2}\left[3e\sin f - \frac{1}{2}\sin 2\theta - \frac{1}{2}e\sin(f+2\omega) - \frac{1}{6}e\sin(3f+2\omega)\right] \tag{17}$$

The same process is followed for the other orbital elements.

To transform a set of elements from mean to osculating the following method is used:

$$e_{osc} = e_{mean} + \varepsilon(\Delta e^{lp} + \Delta e^{sp1} + \Delta e^{sp2}) \tag{18}$$

Where e is $\left[a\ \theta\ i\ q_1\ q_2\ \Omega\right]^T$ and $\varepsilon = -J_2R_e^2$. The long period variation due to Earth oblateness, Δe^{lp}, and the short period variations, $\Delta e^{sp1}, \Delta e^{sp2}$, can be determined from the preceding development. The exact formulation used for this paper is from Alfriend and Gim[10], based on work by Brouwer[11] and Lydanne[12]. The equations used are listed in Appendix I.

E. Secular Effects

In addition to the periodic perturbations, the Mean anomaly, M, the Argument of Perigee, ω, and the RAAN experience secular changes. These angular rates are obtained from general perturbation theory:

$$\begin{aligned}
\dot{\Omega} &= -1.5J_2n\left(\frac{R_e}{p}\right)^2\cos i \\
\dot{\omega} &= 0.75J_2n\left(\frac{R_e}{p}\right)^2\left(5\cos^2 i - 1\right) \\
\dot{M} &= n + 0.75J_2n\left(\frac{R_e}{p}\right)^2\sqrt{1-e^2}\left(3\cos^2 i - 1\right)
\end{aligned} \tag{19}$$

Therefore the time-varying mean elements are

$$\begin{aligned} a(t) &= a_0 \\ \theta(t) &= \theta_0 + \dot{\theta}t \\ i(t) &= i_0 \\ q_1(t) &= q_{1_0} \\ q_2(t) &= q_{2_0} \\ \Omega(t) &= \Omega_0 + \dot{\Omega}(t) \end{aligned} \tag{20}$$

As described above, the osculating elements are obtained by adding the periodic terms to these mean elements.

For this paper, an orbital period is defined as the time it takes for the deputy to travel through 2π radians in the precessing orbital plane. As such, we will also define the mean motion of the satellite to be its perturbed mean motion, in other words, the mean motion will be equal to the unperturbed mean motion plus the secular rate of change of the mean anomaly due to J_2, as seen in Eqs (19). This allows for the mean motion to account for the secular changes to the Mean anomaly due to Earth oblateness.

CHAPTER 4. OBLATENESS EFFECTS ON RELATIVE TRAJECTORY

A. Effects on an In-plane Formation

The largest effect of the oblateness perturbation is an induced drift in the relative trajectory. To see this, a relative formation is set up with one chief and one deputy. The initial orbital elements of the chief are:

$$a= 7378 \text{ km}, \theta=0, i=50 \text{ deg}, q_1=0, q_2=0, \Omega=0 \text{ deg}$$

The initial relative orbital elements for the deputy are:

$$a_e= 500 \text{ m}, \ x_d=0, \ y_d=0, z_{max}=0, \gamma=0 \text{ deg}, \beta=0 \text{ deg}$$

This is considered to be an "in-plane" formation because the relative ellipse is in the plane of the orbit. This is indicated by $z_{max}=0$. These conditions are used to determine the initial conditions of the deputy using Eqs (1) and the processes outlined in Chapter 2. The states of the two satellites are then propagated forward in time using Eqs (7), which include oblateness perturbations. A Runge-Kutta variable step size numerical integrator in MATLAB is used for the simulation. The results are shown in Figure 4 for a time period of 10 orbits and indicate a drift on the order of five meters per orbit. This is problematic for a station-keeping scheme in that the satellite would constantly be fighting drift to remain in a nominal relative orbit.

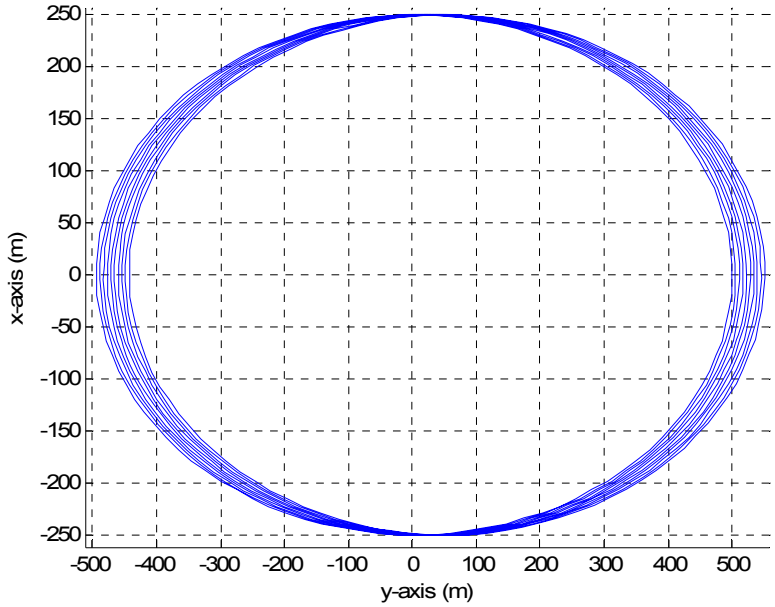

Figure 4: Relative Formation Drift

B. Effects on an Out-of-plane Formation

This effect is also seen in an out-of-plane formation. To illustrate this, the same initial conditions for the chief will be used. For the deputy, all relative orbital elements will remain the same with the exception of z_{max}. For this example, z_{max}=500 m to achieve out-of-plane relative motion. The results are seen in Figure 5. This formation has a drift on the order of fourteen meters per orbit.

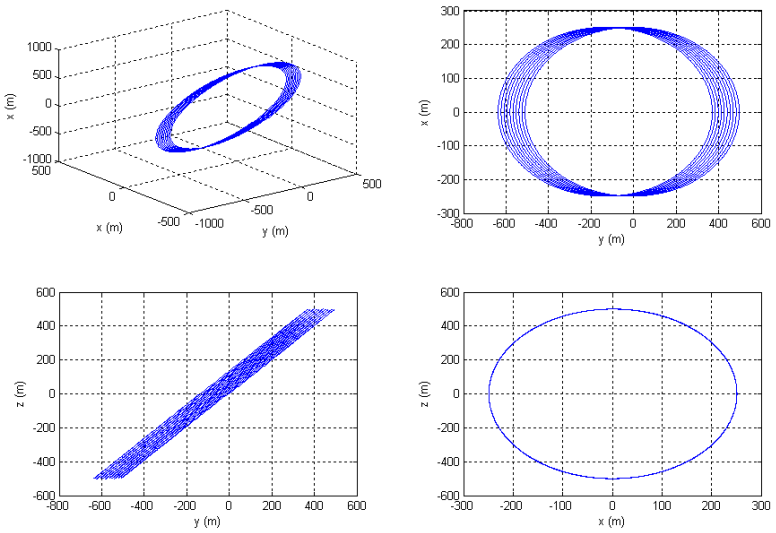

Figure 5: Oblateness Effects on Out-of-Plane Motion

CHAPTER 5. J_2 INVARIANT RELATIVE ORBITS

A. Orbital Element Initialization

Eliminating drift in relative orbits requires several steps. The first step is to consider the initial orbital elements of both the chief and the deputy to be mean elements and then convert them to osculating elements. Doing this allows for the periodic oscillations of the elements to be taken into account when initializing a formation. Care needs to be taken in choosing which method to use to transform your elements. Small errors can lead to bad initial conditions for the formation. The process used for this paper is outlined in Chapter II. For the rest of this paper, when discussing formation design, all orbital elements are assumed to be mean orbital elements.

B. Matching Periods and Nodal Precession Rates

As mentioned in Chapter III, Earth oblateness causes secular change in an orbit's mean anomaly, argument of perigee, and RAAN. Differences in these rates between a chief and a deputy cause unwanted drift in a formation. To negate this effect, we perturb the deputy's orbit to match the period and nodal precession rate. These two conditions are what are referred to as the J_2 invariant orbit in Ref. 2. They are expressed as:

$$\begin{aligned} \dot{\Omega}_c &= \dot{\Omega}_d \\ \dot{\theta}_c &= \dot{M}_c + \dot{\omega}_c = \dot{\theta}_d \end{aligned} \tag{21}$$

The subscripts of "c" and "d" refer to the chief and deputy, respectively. Formulas for the angular rates are from Eq (18).

To match the period and nodal precession, we take the variation of Eqs (19). Problems arise for circular chief orbits because the terms accompanying eccentricity will drop out of the equations. Therefore, as in Ref. 13, we define the new variable:

$$\eta = \sqrt{1-e^2} \tag{22}$$

Also, for convenience, we define

$$C = \frac{3J_2 {R_e}^2 n}{2a^2\eta^4} \tag{23}$$

Taking the variation of Eqs (19) gives us:

$$\begin{aligned}
\delta(\dot{M}+\dot{\omega}) &= \delta\left[n + C(1-\tfrac{3}{2}\sin^2 i)\eta + C(\tfrac{5}{2}\cos^2 i - \tfrac{1}{2})\right] \\
&= -\tfrac{1}{2a}\left[3n + 7C(1-\tfrac{3}{2}\sin^2 i)\eta + 7C(\tfrac{5}{2}\cos^2 i - \tfrac{1}{2})\right]\delta a \\
&\quad - C\left[3(1-\tfrac{3}{2}\sin^2 i) + \tfrac{4}{\eta}(\tfrac{5}{2}\cos^2 i - \tfrac{1}{2})\right]\delta\eta - C\cos i \sin i(3\eta+5)\delta i \\
\delta\dot{\Omega} &= \delta\left(-C\cos i\right) = \tfrac{7C}{2a}\cos i\,\delta a + \tfrac{4C}{\eta}\cos i\,\delta\eta + C\sin i\,\delta i
\end{aligned} \tag{24}$$

where the orbital elements are mean chief elements. Using Eqs (24), it is then possible to determine a relative deputy orbit that will not drift.

C. Designing a Relative Orbit

To aid in designing a relative trajectory that does not drift, we have reformulated Eqs (24) in terms of relative orbital elements. To do this, we first need to take the variation of Eq (22). We define

$$\delta\eta = \eta_d - \eta_c \tag{25}$$

Then we use Eq (22) and the fact that our chief is circular to get

$$\delta\eta = \sqrt{1-e_d^2} - 1 \tag{26}$$

Since our chief is circular we can use the substitution

$$e_d = \delta e \tag{27}$$

to change Eq (26) to the form

$$\delta\eta = \sqrt{1-\delta e^2} - 1 \tag{28}$$

and finally use a binomial series expansion to reach the equation

$$\delta\eta \approx -\tfrac{1}{2}\delta e^2 \tag{29}$$

We then make use of a linear conversion between orbit element differences and relative orbit elements of

$$\begin{aligned} \delta a &= x_d \\ \delta i &= \frac{z_{\max}}{a}\cos\left(\theta-\left(\gamma+\beta\right)\right) \\ \delta e &= \frac{a_e}{2a} \end{aligned} \tag{30}$$

to get Eqs (24) in terms of relative orbit elements.

$$\begin{aligned} \delta(\dot{M}+\dot{\omega}) = &-\tfrac{1}{2a}\left[3n+7C(1-\tfrac{3}{2}\sin^2 i)\eta+7C(\tfrac{5}{2}\cos^2 i-\tfrac{1}{2})\right]x_d \\ &+\tfrac{C}{8a^2}\left[3(1-\tfrac{3}{2}\sin^2 i)+\tfrac{4}{\eta}(\tfrac{5}{2}\cos^2 i-\tfrac{1}{2})\right]a_e{}^2 \\ &-\tfrac{C}{a}\cos i\sin i(3\eta+5)\, z_{\max}\cos\left[\theta-(\gamma+\beta)\right] \\ \delta\dot{\Omega} = &\tfrac{7C}{2a}\cos i\, x_d-\tfrac{C}{2\eta a^2}\cos i\, a_e{}^2+\tfrac{C}{a}\sin i\, z_{\max}\cos\left[\theta-(\gamma+\beta)\right] \end{aligned} \tag{31}$$

This formulation allows for one of the set of relative elements and element combinations {x_d, a_e^2, $z_{max}\cos[\theta-(\gamma+\beta)]$} to be fixed and determine the other two from the linear system of equations above. These J_2 invariant relative orbit elements can then be used to determine the orbital elements of the deputy.

For example, the designer may wish to consider various values of γ and look at the values of x_d and a_e take on for J_2 invariance. These relationships are shown in Figure 6 for a z_{max} of 50 meters. Note that for a value of $\pi/2$ that a_e becomes very small. This is because there is no inclination difference between the deputy and the chief for this value of γ.

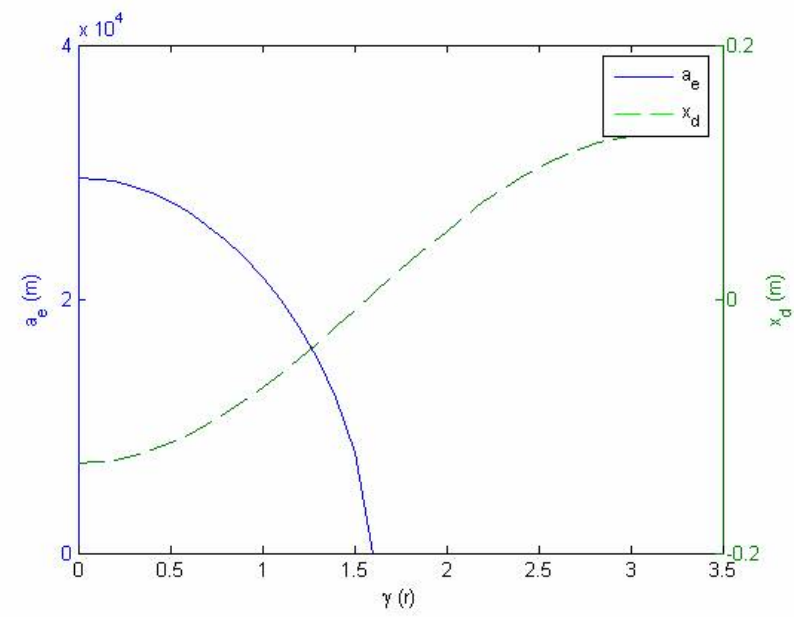

Figure 6: Conditions for J_2 Invariance with Varying γ

For an out-of-plane formation, problems occur due to the semi major axis squared in the denominator of the a_e term in Eqs (31). This makes the coefficient of a_e very small, so large changes in a_e are necessary of any non-negligible change in the other relative orbital elements. Thus, matching both the period and the nodal rates for significant z_{max} with relatively small a_e values (kilometers or less) is physically impossible. As seen if Figure 6, for relatively small values of z_{max}, the value of a_e increases dramatically. Therefore, in this report we will only match the period between the deputy and the chief. The repercussions of this will be seen in the following section.

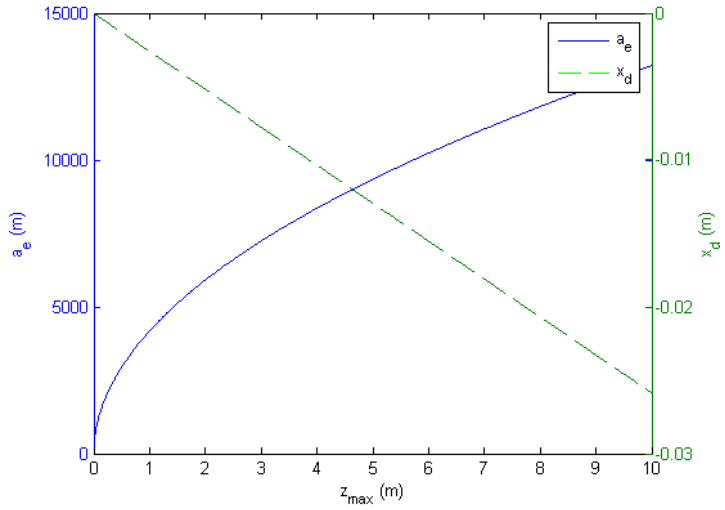

Figure 7: Various Conditions for J_2 Invariance with Varying z_{max}

To demonstrate the effectiveness of period and nodal rate matching we consider both an in-plane and out-of-plane example. For the in-plane example, solving Eqs (31), gives the following relative orbital elements for the deputy:

$$a_e = 500 \text{ m}, \; x_d = -3.7 \times 10^{-5} \text{ m}, \; y_d = 0, \; z_{max} = 3 \times 10^{-16}, \; \gamma = 0 \text{ deg}, \; \beta = 0 \text{ deg}$$

Notice that the values for x_d and z_{max} are very close to the original values. Because there is no inclination difference between the chief and the deputy, the period and nodal rate matching conditions are very nearly met by simply setting $x_d = 0$.

These equations are useful in designing and analyzing a relative orbit. However, using these linear conversions to initialize an orbit leads to unnecessary error in the solution. Instead, Eqs (21) are used directly to initialize the orbit. Doing so leads to the following initial orbital elements for the deputy:

$$a = 7378999.999963 \text{ m}, \; \theta = 0 \text{ deg}, \; i = 50 \text{ deg}, \; q_1 = 3.389 \times 10^{-5}, \; q_2 = 0, \; \Omega = 0 \text{ deg}$$

For these orbital elements to produce a J_2 invariant orbit, they are considered to be mean orbital elements. Utilizing the mean to osculating conversion gives the following initial osculating orbital elements for the chief and the deputy:

$$a_c = 7383251.179 \text{ m}, \; \theta_c = 0 \text{ deg}, \; i_c = 50.0171 \text{ deg}, \; q_{1c} = 7.384 \times 10^{-4}, \; q_{2c} = 0, \; \Omega_c = 0 \text{ deg}$$
$$a_d = 7383251.786 \text{ m}, \; \theta_d = 0 \text{ deg}, \; i_d = 50.0171 \text{ deg}, \; q_{1d} = 7.723 \times 10^{-4}, \; q_{2d} = 0, \; \Omega_d = 0 \text{ deg}$$

Using the MATLAB simulation previously described, the relative trajectory created by using these initial conditions is seen in Figure 8. The drift from Figure 4 is completely negated by the mean to osculating conversion. Over the 100 orbits graphed, the drift in the formation is only .9 m, or 9 millimeters per orbit.

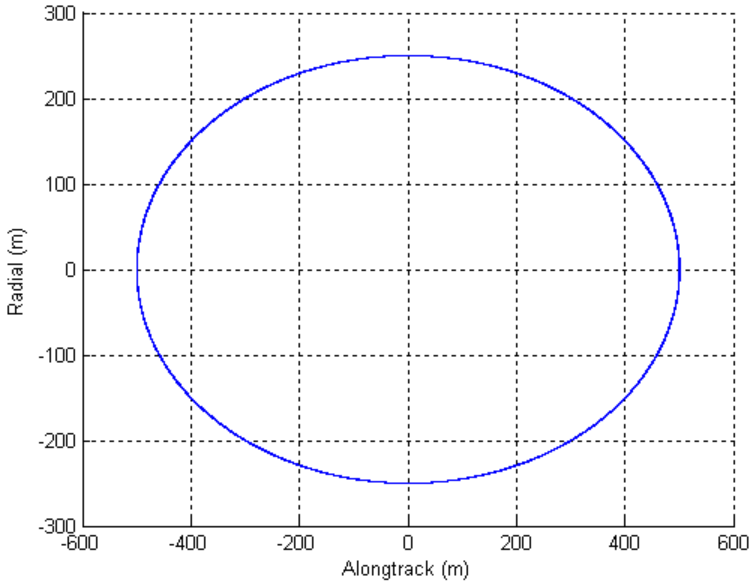

Figure 8: In-plane J_2 Invariant Relative Trajectory (100 Orbits)

For the out-of-plane example, as mention above we cannot find a fully J_2 invariant orbit, so we only match the period. Specifying two of the three relative orbit parameters in the period matching equation in Eqs (31) will allow for an out-of-plane formation that has reduced drift versus its non-matched counterpart. Using this method for an out-of-plane formation yields the following initial relative orbital elements:

$$a_e = 500 \text{ m}, \quad x_d = -1.590 \text{ m}, \quad y_d = 0, \quad z_{max} = 500 \text{ m}, \quad \gamma = 0 \text{ deg}, \quad \beta = 0 \text{ deg}$$

The perturbation to x_d is much larger than that of the in-plane formation. Using these initial conditions to simulate the relative formation leads to the relative trajectory in Figure 9. The drift of this formation is greatly reduced from that of the trajectory in Figure 5.

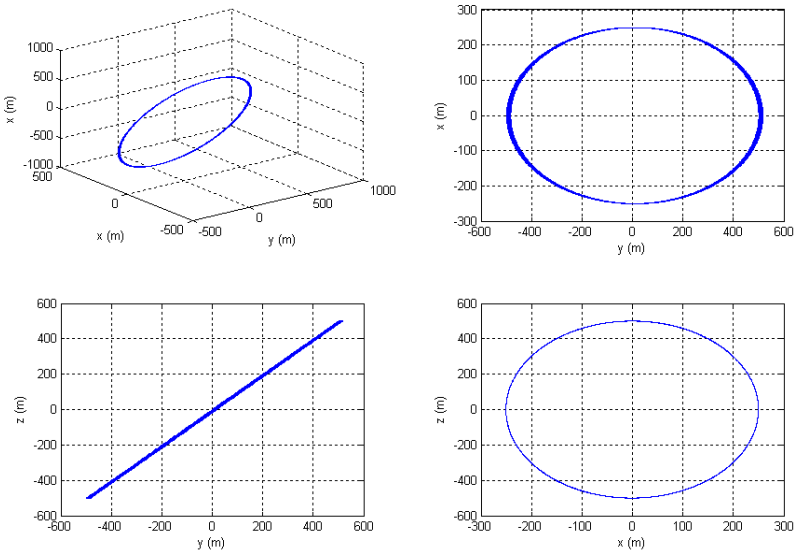

Figure 9: Out-of-Plane Period Matching – 10 Orbits

This reduction in drift from an unmatched trajectory will keep the formation from fighting the full effects of drift caused by J_2. Even so, there is still drift in the formation of about 1.84 meters per orbit. This is caused by the unmatched differential secular rate of change between the RAAN of the chief and the deputy. The differential nodal rate causes in-plane drift to occur as discussed in the next section.

D. Drift Due to Differential Nodal Rates

To characterize this drift, assume that the chief and the deputy are collocated. We can do this without loss of generality. With a nearly circular chief and period matching conditions enforced, the chief and the deputy will both recross the equatorial plane at the same time one period later. Over that period of time, *T*, a difference in the RAAN of the two satellites will have occurred. The distance between the chief and the deputy will be given by

$$(\dot{\Omega}_d - \dot{\Omega}_c)Ta_c \tag{32}$$

The component parallel to the orbit plane (see Figure 10) is:

$$\text{Drift} = \Delta\dot{\Omega}Ta\cos i \tag{33}$$

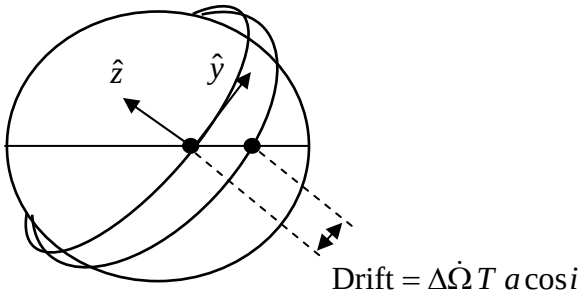

Figure 10: Drift Due to Differential Nodal Rate

Using the example from Figure 9, the calculated drift would be

$$\text{In-plane drift} = (\dot{\Omega}_d - \dot{\Omega}_c) T a_c \cos i_c = 1.88\,\text{m} \tag{34}$$

which matches up nicely with the observed drift seen in Figure 11 of

$$\text{In-plane drift}=(517.3-500.7)/9=1.84\ \text{m} \tag{35}$$

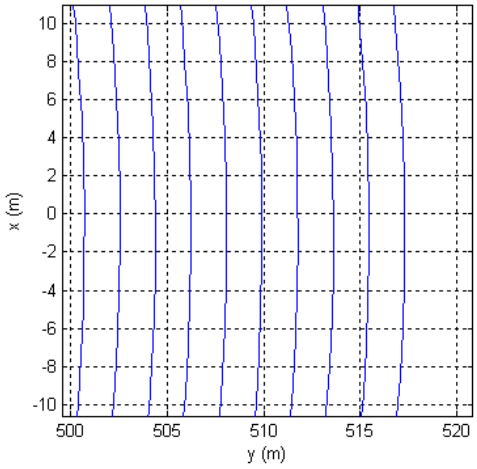

Figure 11: Blow up of Figure 9 to Determine Drift

In addition to the in-plane drift, there is also some out-of-plane motion associated with nodal drift. This motion affects γ and z_{max}.

In the J_2 invariant work by Schaub and Alfriend[2], their process for finding an invariant relative orbit requires defining one of three deputy orbital elements, either semi major axis, eccentricity, or inclination,

and then finding the other two to initialize the relative orbit. The problem with this approach is that the relative orbital elements that define such an orbit are unable to be changed and do not always form a relative orbit that is desired.

For formation design purposes, this approach lacks the ability to define the J_2 invariant orbit that meets the requirements of the formation design. The approach laid out here allows for a relative orbit that not only has close to the desired relative orbital elements, but also reduces drift to an amount that can be corrected by a stationkeeping scheme.

CHAPTER 6. GUIDANCE APPROACH

A. Defining the Nominal Trajectory

For a stationkeeping scheme, two different nominal trajectories need to be defined: the trajectory used to monitor deviation and the target state for a maneuver. Deviations from the nominal will be measured in the relative state. The least computationally intensive solution is to use Eqs (1). This is the trajectory we will use to monitor deviation. When we initialize the formation, we perturb the deputy to create a period matched orbit. When using the parameters to monitor the formation, we will set x_d=0, since the drift has ideally been removed. The mean motion used will be that of the J_2 perturbed mean motion. To propagate forward our relative trajectory, we will propagate forward β to a time T by using:

$$\beta(T) = \beta_o + \dot{M}T \tag{36}$$

For the target state at the end of a maneuver, we will use a slightly different approach. For target conditions, we need to take into account targeting mean elements (versus osculating elements) and we will need to perturb the target to remove any unnecessary drift. We will first propagate forward the mean argument of latitude of the chief. Likewise, the chief's anomaly is propagated forward by simply using the perturbed mean motion:

$$\theta(T) = \theta_o + \dot{M}T \tag{37}$$

In the relative state, the RAAN is ignorable, so it is not updated. The chief orbital elements and the relative orbital elements of the deputy at time T are then used to find the desired orbital elements of the deputy.

To remove unwanted drift, the deputy's mean orbital elements are then perturbed using the period matching process described in Chapter VI. The desired orbital elements of the chief and deputy are then converted to osculating elements. Once these are found, the target state of the deputy is found in a LVLH frame in a process similar to that mentioned in Chapter II, found in standard astrodynamical texts[7]. It is this relative position and velocity that are used for targeting the maneuver.

B. Calculating ΔV for Maneuvering

The nominal trajectory used to determine when the deputy needs to maneuver is the nominal position given by Eqs (1). To measure deviation, the nominal relative position is subtracted from the actual relative position and the magnitude of this position vector is considered the deviation. A radius of a sphere, or deadband, is specified that we want the satellite to remain inside. To determine if a maneuver is warranted, we check the deviation to see if it has reached a certain percentage of that deadband. If it is at that distance or further, we enact a maneuver. Each stationkeeping maneuver consists of two burns. This gives six degrees of freedom to completely match the nominal state. The first maneuver will send the satellite back to a nominal position, $\delta\bar{r}(T)$, where *T* is the time at the end of the maneuver. The maneuver needs to be short enough that several maneuvers can take place per orbit.

To determine the trajectory that will return our satellite to nominal, we will need to develop a state transition matrix for the LVLH frame of reference. We follow the process laid out in Prussing and Conway[14]. Developing the necessary equations requires us to start in an inertial frame of reference, seen in Figure 12.

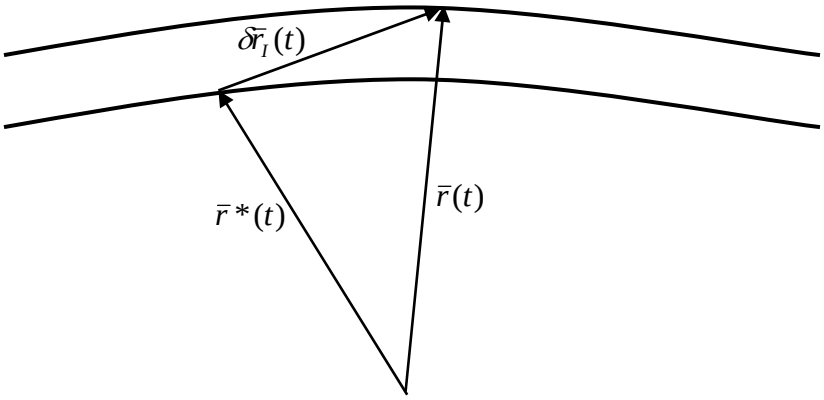

Figure 12: Inertial Frame of Reference

Using the equation of motion in a general gravity field,

$$\ddot{\bar{r}} = g(\bar{r}) \tag{38}$$

along with the relationship of

$$\bar{r} = \bar{r}^* + \delta\bar{r}_I \tag{39}$$

we are able to get a series expansion of the equation of motion in a general gravity field

$$\ddot{\bar{r}}^* + \delta\ddot{\bar{r}}_I = g(\bar{r}^* + \delta\bar{r}_I) = g(\bar{r}^*) + \frac{\delta g(\bar{r}^*)}{\delta \bar{r}^*}\delta\bar{r}_I + \mathcal{O} \tag{40}$$

where the higher order terms are ignorable due to the large difference in size between the position of the chief and $\delta\bar{r}_I$. Using this equation and the fact that the reference orbit satisfies the equations of motion gives us a linear differential equation for our relative trajectory given in Eq (41).

$$\delta\ddot{\bar{r}}_I = \frac{\delta g(\bar{r}^*)}{\delta \bar{r}^*}\delta\bar{r}_I = G(\bar{r}^*)\delta\bar{r}_I \tag{41}$$

To make this equation specific to our application, we use the inverse square gravitational force equation

$$G(\bar{r}) = \frac{\mu}{r^5}(3\bar{r}\bar{r}^T - r^2 I_3) \tag{42}$$

along with the relationships

$$\bar{r}^* = \begin{bmatrix} r^* \\ 0 \\ 0 \end{bmatrix}, \quad n^2 = \frac{\mu}{r^{*3}} \tag{43}$$

to get the specific equations of motion in an inertial frame of

$$\delta\ddot{\bar{r}}_I = n^2 \begin{bmatrix} 2 & 0 & 0 \\ 0 & -1 & 0 \\ 0 & 0 & -1 \end{bmatrix} \delta\bar{r}_I \tag{44}$$

Next, we need to convert this equation into the rotating LVLH frame. To do this, we will use the acceleration expansion

$$\delta\ddot{\bar{r}} = \delta\ddot{\bar{r}}_I - 2\bar{\omega} \times \delta\dot{\bar{r}} - \dot{\bar{\omega}} \times \delta\bar{r}_I - \bar{\omega} \times (\bar{\omega} \times \delta\bar{r}_I) \tag{45}$$

to get the equations of motion in the proper frame. The angular rate, $\bar{\omega}$, is defined as

$$\omega = \begin{bmatrix} 0 \\ 0 \\ n \end{bmatrix} \tag{46}$$

Assuming constant mean motion gives

$$\begin{aligned} \ddot{x} &= 3n^2 x + 2n\dot{y} \\ \ddot{y} &= -2n\dot{x} \\ \ddot{z} &= -n^2 z \end{aligned} \tag{47}$$

These equations are the Clohessy-Wiltshire equations. To get the state transition matrix for relative position and velocity, these differential equations are integrated to get

$$\begin{aligned} x(t) &= (4-3\cos nt)x_0 + \frac{\sin nt}{n}\dot{x}_0 + \frac{2}{n}(1-\cos nt)\dot{y}_0 \\ y(t) &= 6(\sin nt - nt)x_0 + y_0 - \frac{2}{n}(1-\cos nt)\dot{x}_0 + \frac{4\sin nt - 3nt}{n}\dot{y}_0 \\ z(t) &= z_0 \cos nt + \frac{\dot{z}_0}{n}\sin nt \\ \dot{x}(t) &= (3n\sin nt)x_0 + (\cos nt)\dot{x}_0 + (2\sin nt)\dot{y}_0 \\ \dot{y}(t) &= -6(1-\cos nt)x_0 - (2\sin nt)\dot{x}_0 + (4\cos nt - 3)\dot{y}_0 \\ \dot{z}(t) &= -z_0 n\sin nt + \dot{z}_0 \cos nt \end{aligned} \tag{48}$$

The terms are then put into a state transition matrix with the form

$$X(t) = \Phi X(t_0) \tag{49}$$

where

$$X = \begin{bmatrix} \delta r \\ \delta \dot{r} \end{bmatrix} \tag{50}$$

This state transition matrix can then be partitioned into the form

$$\Phi = \begin{bmatrix} \Phi_{rr} & \Phi_{rv} \\ \Phi_{vr} & \Phi_{vv} \end{bmatrix} \tag{51}$$

These partitions can then be used to determine what velocity would be needed to maneuver to a certain position after a certain time period by the equation

$$\Delta V_1 = \Phi_{rv}(T)^{-1}\left[\delta\bar{r}(T) - \Phi_{rr}(T)\delta\bar{r}(0)\right] - \delta\bar{v}(0) \tag{52}$$

where the Φ matrices are partitions of the state transition matrix and $\delta r(0)$ and $\delta v(0)$ are the relative position and velocity at the beginning of the maneuver. The position at the end of maneuver, $\delta\bar{r}(T)$, is determined using the process laid out at the beginning of this chapter.

The second burn in the stationkeeping maneuver removes any velocity relative to the reference so that the deputy stays on the nominal trajectory is simply

$$\Delta V_2 = \delta\bar{v}_{nom}(T) - \delta\bar{v}(T) \tag{53}$$

where $\delta\bar{v}_{nom}(T)$ is determined from the process at the beginning of this chapter.

Due to the assumption that the satellite will have three axis capability and will not have to slew to perform a maneuver, the total ΔV is given by

$$\Delta V = \sum_{i=1}^{2}\sum_{j=1}^{3}\left|\Delta V_{ij}\right| \tag{54}$$

where *i* refers to the first and second burns and *j* refers to the $\hat{x}$, $\hat{y}$, and $\hat{z}$ direction.

CHAPTER 7. MONTE CARLO ANALYSIS

A. Monte Carlo Setup

To evaluate the performance of the stationkeeping scheme, a Monte Carlo analysis is performed for 100 runs of 20 orbits (2000 total orbits). The chief satellite is placed on a perfectly known orbit with a mean eccentricity of zero. The deputy satellite is initially placed on the desired relative formation but then corrupted using the navigation uncertainties. The chief and deputy satellite dynamics are then simulated with a high fidelity propagator that includes nonlinear effects, Earth oblateness, and navigation and control errors. Burns are assumed to be instantaneous and the satellite is assumed to have three axis burn capability. Burn calculations are corrupted using the expected distribution of the thrust magnitude, which is assumed to be Gaussian.

The performance of the satellite will be evaluated based on the number of maneuvers per orbit, the amount of ΔV expended per day, and the time spent within the deadband, "availability". The radius of the deadband is set at three meters. Using this deadband and running short simulations without Earth oblateness, the time spent during a maneuver is set at one quarter of an orbit and the percentage of the deadband at which the maneuver is triggered is set at ninety percent. Using this percentage of the deadband is important because waiting until the satellite is outside of the deadband before a maneuver is started leads to the satellite spending more of its time outside of its deadband and availability suffers greatly.

For the Monte Carlo simulation, the following parameters in Tables 1 and 2 are used.

Table 1
BASELINE ERROR SOURCES

Error Source	Position (mm)	Velocity (mm/s)	Thrust (%)
Value – 1σ	5.0	0.5	5

Table 2
STATIONKEEPING PARAMETERS

Constraint	Deadband (m)	Maneuver Time (orbits)	Threshold (%)
Value	3	0.25	90

B. In-plane Case

The first case analyzed is the in-plane relative formation case. For initialization, the chief satellite's initial mean orbital elements will be:

$$a= 7378 \text{ km}, \theta=0, i=50 \text{ deg}, q_1=0, q_2=0, \Omega=0 \text{ deg}$$

The initial mean relative orbital elements for the deputy are:

$$a_e= 500 \text{ m}, \ x_d=0, \ y_d=0, z_{max}=0, \gamma=0 \text{ deg}, \beta=0 \text{ deg}$$

For comparison purposes, a baseline case is run using only the unperturbed two body equations of motion. The results from this simulation are the optimal results achievable. The goal of the guidance approach is to get the formation results with J_2 perturbations as close to this nominal as possible. The results are in Table 3 and Figure 13 shows a histogram of the number of maneuvers, ΔV per day, and percent of time spent within the deadband.

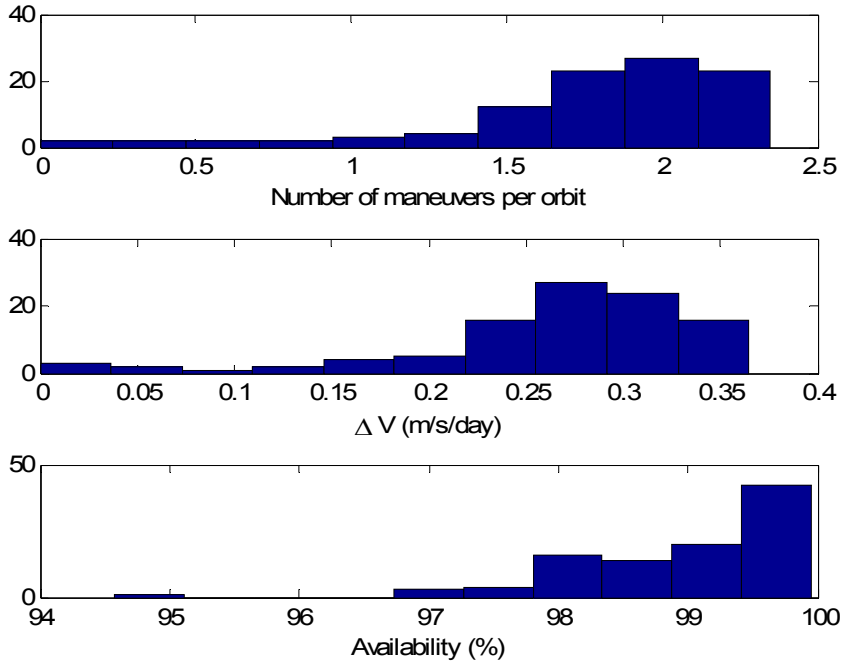

Figure 13: Histogram of Baseline Case

Table 3
BASELINE RESULTS

	Within Deadband	ΔV (m/s/day)	Num. Maneuvers per orbit
Mean	99.0%	0.264	1.752
Std. Deviation	0.9%	0.077	0.487

To gauge the efficiency of our stationkeeping approach, the Monte Carlo simulation is run that includes J_2 in the simulation dynamics, but not in the guidance. Instead, it employs the maneuver scheme used in a recent AFRL study[15] (which is based on the standard unperturbed dynamics). As can be seen in Table 4 and Figure 14, the results from this simulation are heavily affected by Earth oblateness. Both the amount of ΔV and the number of maneuvers have increased. The availability is also significantly reduced.

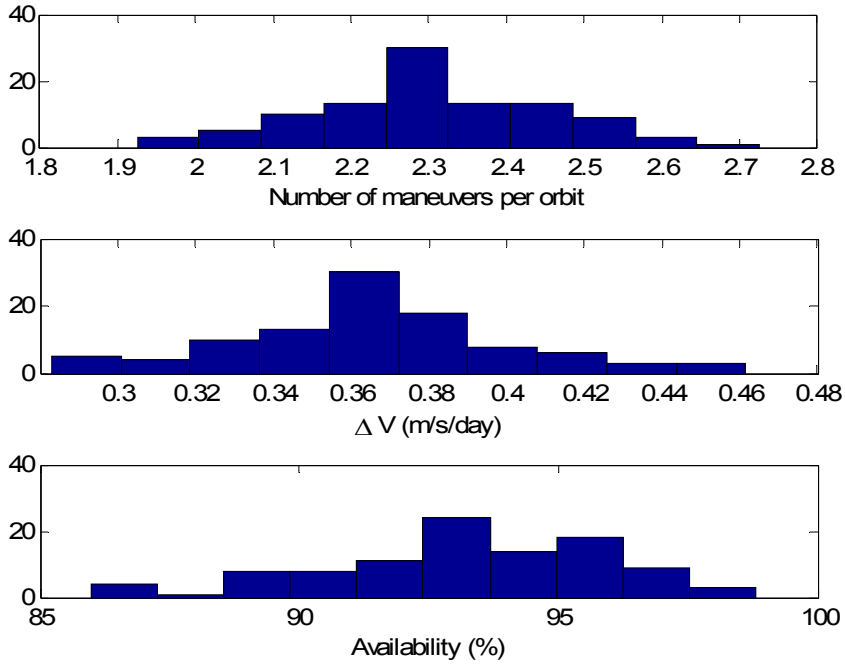

Figure 14: Histogram of In-plane Case with Earth Oblateness

Table 4
RESULTS WITH EARTH OBLATENESS

	Within Deadband	ΔV (m/s/day)	Num. Maneuvers per orbit
Mean	93.2%	0.365	2.308
Std. Deviation	2.7%	0.036	0.152

Finally, for the in-plane case, we include our maneuver scheme which incorporates the J_2 perturbations into the guidance to minimize the effect of Earth oblateness. The previous two examples for the in-plane case used simple CWH equations in their maneuver schemes and used the unperturbed mean motion. It can be seen from the results in Table 5 that using our maneuver scheme and using the perturbed mean motion allows for the performance of this scheme to be greatly improved over that of the previous case. The performance is not as good as the baseline, but the guidance approach that we have developed greatly mitigates the impact J_2 has on the formation maintenance.

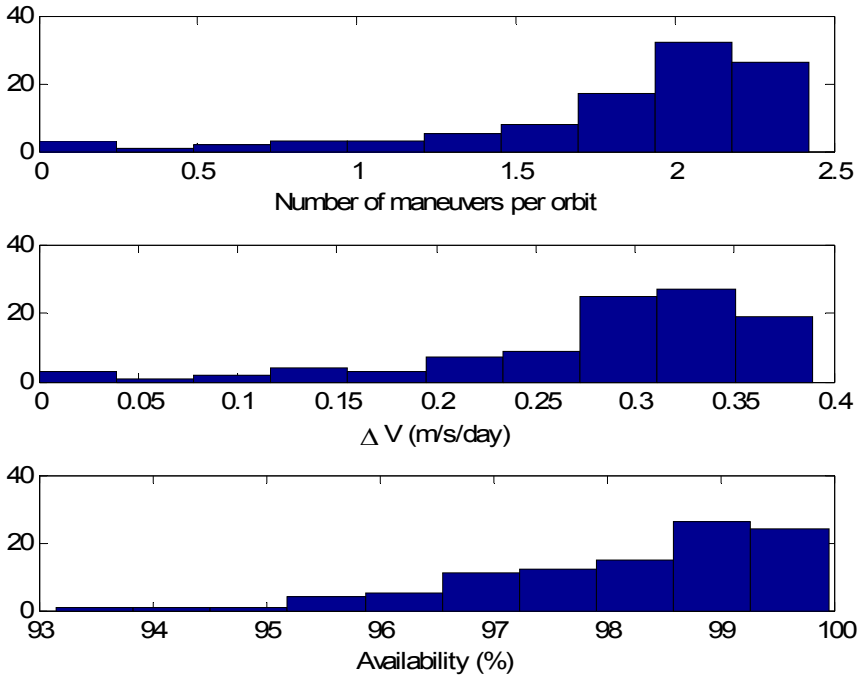

Figure 15: Histogram of In-plane Case with New Guidance

Table 5
IN-PLANE RESULTS WITH NEW GUIDANCE

	Within Deadband	ΔV (m/s/day)	Num. Maneuvers per orbit
Mean	98.2%	0.284	1.829
Std. Deviation	1.4%	0.085	0.528

C. Out-of-plane Case

For the out-of-plane formation, the same initial conditions are used, with the exception that z_{max}=500 for this formation. A baseline case (with the simple unperturbed dynamic model) is run for the out-of-plane formation and the results are in Table 6 and Figure 16. The results are very similar to the in-plane case.

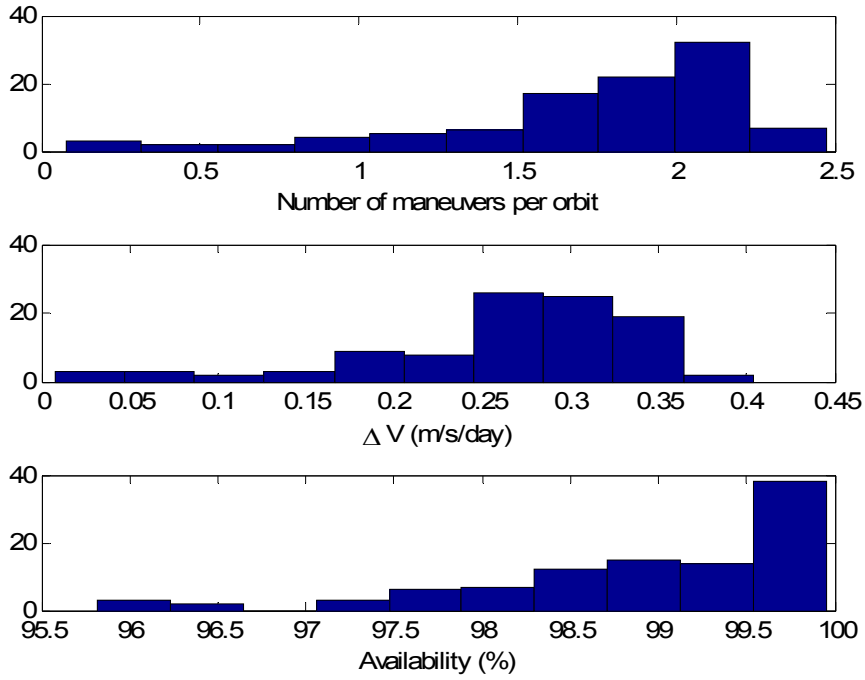

Figure 16: Histogram of Baseline Case

Table 6
OUT-OF-PLANE BASELINE

	Within Deadband	ΔV (m/s/day)	Num. Maneuvers per orbit
Mean	99.0%	0.262	1.746
Std. Deviation	1.0%	0.081	0.512

The next case run uses the same maneuver scheme as the baseline but now we include J_2 perturbations in the equations of motion (but not in the guidance scheme). The results are found in Table 7 and Figure 17. The performance is seriously degraded due to the perturbations. The number of maneuvers has significantly increased as well as the ΔV and the availability has dropped by just under thirty percent.

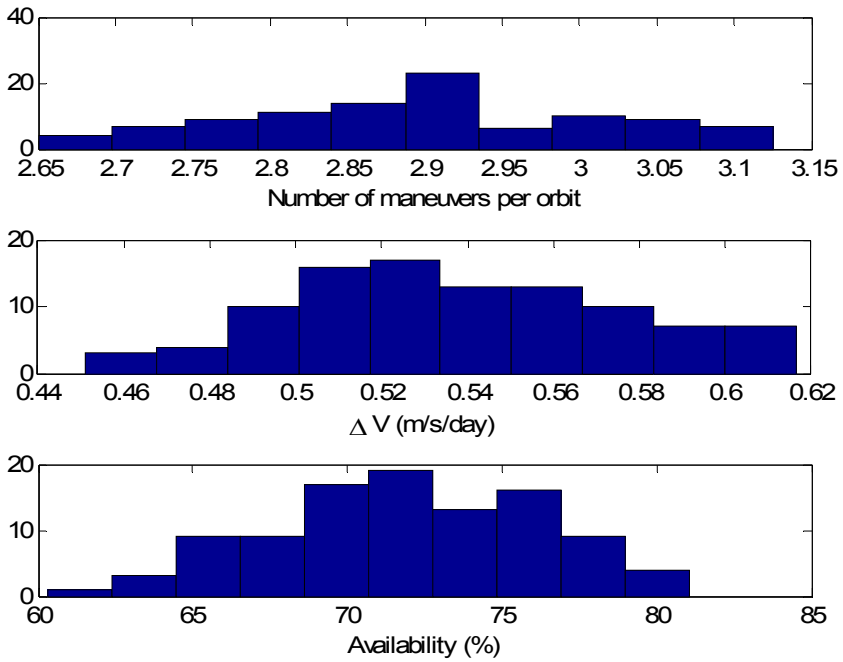

Figure 17: Histogram of Out-of-Plane with Perturbations

Table 7
OUT-OF-PLANE WITH PERTURBATIONS

	Within Deadband	ΔV (m/s/day)	Num. Maneuvers per orbit
Mean	71.9%	0.537	2.899
Std. Deviation	4.3%	0.038	0.123

Next the new guidance scheme with J_2 effects is employed in the simulation. The results are improved over the previous case. Availability is increased by seventeen percent over the unmatched case and the ΔV requirements and the number of maneuvers are decreased by thirty-five percent and twenty-five percent, respectively. The results are found in Table 8 and Figure 18.

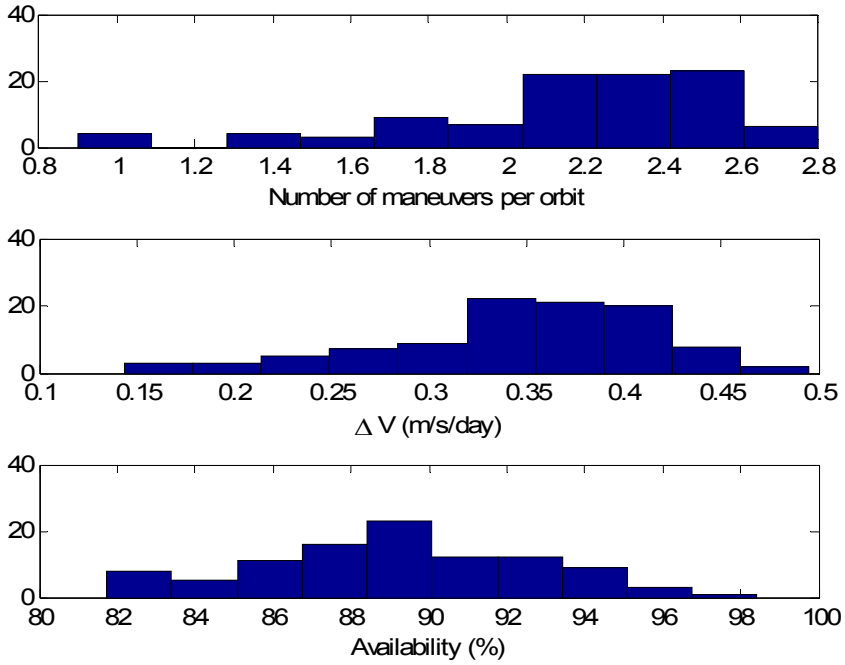

Figure 18: Out-of-Plane with Oblateness and New Guidance

Table 8
OUT-OF-PLANE WITH OBLATENESS AND NEW GUIDANCE

	Within Deadband	ΔV (m/s/day)	Num. Maneuvers per orbit
Mean	89.2%	0.348	2.167
Std. Deviation	3.5%	0.073	0.408

To assess the relative merits of the different features of the new guidance scheme, we run a case without period matching. The J_2 effects are still partially accounted for in this case by using the perturbed mean motion in the calculation of the nominal trajectory. The results are shown in Table 9. The performance is

better than the case with no J_2 in the guidance (Table 7) but worse than the fully developed scheme (Table 8). This shows that both period matching and the modifications to the CWH equations are important in the improvement of the performance over previous approaches.

Table 9
OUT-OF-PLANE WITH OBLATENESS WITHOUT PERIOD MATCHING

	Within Deadband	ΔV (m/s/day)	Num. Maneuvers per orbit
Mean	87.9%	0.379	2.337
Std. Deviation	4.3%	0.064	0.339

D. Summary of Results

The effects of J_2 are significant for relative orbits in a low Earth orbit. Using the maneuver scheme presented in this report, with period matching and using a perturbed mean motion calculation, brings the performance of the formation back close to the baseline case. The results for the in-plane case with the maneuver scheme are very close to that of the baseline. The out-of-plane results are improved from the case with perturbations but are not quite at baseline due to the drift caused by the differential nodal rate.

The process presented in this report allows for very tight control of a relative trajectory using several stationkeeping burns per orbit. When J_2 is accounted for, the process helps to minimize the amount of ΔV required to keep the deputy near its nominal position.

CHAPTER 8. FUTURE WORK

The maneuver scheme laid out in the paper helps to reduce the effects of J_2 on the stationkeeping performance of a satellite maintaining a relative trajectory. However, this approach has not quite gotten the number of maneuvers, ΔV, and availability back to values similar to the baseline cases. The next step would be to add J_2 guidance into state transition matrix for the calculation of the station-keeping burn. Currently, the maneuver state transition matrix is based off of the two body equations of motion and does not take into account J_2. Using a J_2 relative state transition matrix should help to move the simulation results closer to the baseline cases. An attempt was made to accomplish this work, but the current development of state transition matrices with J_2 did not seem to have the sufficient accuracy for this application. This area merits further investigation.

Another next step in the research would be to account for uncertainty and eccentricity in the chief trajectory. Currently, the chief is presumed to be perfectly known and circular. The chief will have some error in the knowledge of its position and velocity and this will also affect ΔV and the maneuver scheme. Eccentricity in the chief orbit will affect the relative orbit also.

REFERENCES

1. C. Sabol, R. Burns, and C. McLaughlin, “Satellite Formation Flying Design and Evolution”, *Journal of Spacecraft and Rockets*, Vol. 38, No. 2, 2001, pp. 270-278.
2. H. Schaub and K.T. Alfriend, “J_2 Invariant Reference Orbits for Spacecraft Formations,” *Celestial Mechanics and Dynamical Astronomy*, Vol. 79, 2001, pp. 77-95.
3. H. Schaub and K.T. Alfriend, “Impulsive Feedback Control to Establish Specific Mean Orbital Elements of Spacecraft Formations,” *Journal of Guidance, Control, and Dynamics*, Vol. 24, No. 4, 2001, pp. 739-745.
4. S. D’Amico and O. Montenbruck, “Proximity operations of formation-flying spacecraft using an eccentricity/inclination vector separation,” *Journal of Guidance, Control and Dynamics*, Vol. 29, No. 3, May/June 2006, pp. 554-563.
5. W.E. Wiesel, “Optimal Impulsive Control of Relative Satellite Motion,” *Journal of Guidance, Control and Dynamics,*Vol 26, No. 1, 2003, pp. 74-78.
6. T.A. Lovell, S.G. Tragesser, M.V. Tollefson, “A Practical Guidance Methodology for Relative Motion of LEO Spacecraft Based on the Clohessy-Wiltshire Equations,” AAS Paper 04-252, AAS/AIAA Space Flight Mechanics Meeting, Maui, Feb 8-12, 2004.
7. D. Vallado, *Fundamentals of Astrodynamics and Applications*, Microcosm Press, El Segundo, CA, 2004.
8. Y. Kozai, “The Motion of a Close Earth Satellite,” *The Astronomical Journal*, Vol. 64, No. 1274, 1959, pp. 367-377.
9. F. Tisserand, *Traite de mechanique celeste*, Gauthier-Villars, Paris, 1889.
10. D.W. Gim and K. T. Alfriend, "The State Transition Matrix of Relative Motion for the Perturbed Non-Circular Reference Orbit," AAS Paper 01-222, AAS/AIAA Space Flight Mechanics Meeting, Santa Barbara, CA, Feb 11-16, 2001.
11. D. Brouwer, “Solutions of the Problem of Artificial Satellite Theory Without Drag,” *The Astronomical Journal*, Vol. 64, No. 1274, 1959, pp. 378-397.
12. R.H. Lydanne, “Small Eccentricities or Inclinations in the Brouwer Theory of the Artificial Satellite,” *The Astronomical Journal*, Vol. 68, October 1963, pp. 555-558.
13. H. Schaub and J.L. Junkins, *Analytical Mechanics of Space Systems*, American Institute of Aeronautics and Astronautics, Inc., Reston, VA, 2003. pp. 628-667.
14. B.A. Conway and J.E. Prussing, *Orbital Mechanics*, Oxford University Press, New York, 1993, pp. 139-152.
15. S. Tragesser, “Error Analysis of a Leader-Follower Satellite Formation,” Air Force Research Laboratory Technical Report, AFRL-VS-PS-TR-2005-1225, November 2005.
16. S.G. Tragesser and B. Skrehart, "Stationkeeping Analysis for Satellite Formations Including Oblateness Perturbations," AAS Paper 07-035, AAS Guidance and Control Conference, Breckenridge, CO, Feb 3-7, 2007.

APPENDIX I. PERIODIC VARIATIONS IN ORBIT ELEMENTS

From Ref. 10:

$$\Theta = (1 - 5\cos^2 i)^{-1}$$

$$a^{lp} = 0$$

$$\theta^{lp} = -\left(\frac{\sin^2 i}{8a^2}\right)\left(1 - 10\Theta\cos^2 i\right)\left(q_1 \sin\theta + q_2 \cos\theta\right)$$

$$i^{lp} = 0$$

$$q_1{}^{lp} = -\left(\frac{q_1 \sin^2 i}{16a^2}\right)\left(1 - 10\Theta\cos^2 i\right)$$

$$q_2{}^{lp} = \left(\frac{q_2 \sin^2 i}{16a^2}\right)\left(1 - 10\Theta\cos^2 i\right)$$

$$\Omega^{lp} = 0$$

$$a^{sp1} = \frac{3}{2aR_e}\left(1 - 3\cos^2 i\right)\left(q_1 \cos\theta + q_2 \sin\theta\right)$$

$$\theta^{sp1} = \frac{9}{4a^2}\left(1 - 5\cos^2 i\right)\left(q_1 \sin\theta - q_2 \cos\theta\right)$$

$$i^{sp1} = 0$$

$$q_1{}^{sp1} = \frac{3\left(1 - 3\cos^2 i\right)}{8a^2}\left(2\cos\theta + 2q_1 + q_1 \cos 2\theta + q_2 \sin 2\theta\right)$$

$$q_2{}^{sp1} = \frac{3\left(1 - 3\cos^2 i\right)}{8a^2}\left(2\sin\theta + 2q_2 + q_1 \sin 2\theta - q_2 \cos 2\theta\right)$$

$$\Omega^{sp1} = \frac{9\cos i}{2a^2}\left(q_1 \sin\theta - q_2 \cos\theta\right)$$

$$a^{sp2} = -\frac{3\sin^2 i}{2aR_e}\left(1+3q_1\cos\theta+3q_2\sin\theta\right)\cos 2\theta$$

$$\theta^{sp2} = \frac{3\left(2-5\cos^2 i\right)}{8a^2}\sin 2\theta + 3\left(\frac{4-9\sin^2 i}{16a^2}\right)\left(q_1\sin\theta - q_2\cos\theta\right)$$
$$+\left(\frac{4-17\sin^2 i}{16a^2}\right)\left(q_1\sin 3\theta - q_2\cos 3\theta\right)$$
$$-\left(\frac{\sin^2 i}{16a^2}\right)\left[-16\sin 2\theta + 7\left(q_1\sin\theta + q_2\cos\theta\right) - 13\left(q_1\sin 3\theta - q_2\cos 3\theta\right)\right]$$

$$i^{sp2} = -\left(\frac{\sin^2 i}{8a^2}\right)\left[3\cos 2\theta + 3\left(q_1\cos\theta - q_2\sin\theta\right) + \left(q_1\cos 3\theta + q_2\sin 3\theta\right)\right]$$

$$q_1{}^{sp2} = \frac{3q_2\left(3-5\cos^2 i\right)}{8a^2}\sin 2\theta + \left(\frac{\sin^2 i}{8a^2}\right)\left(3\cos\theta - \cos 3\theta\right)$$
$$-\left(\frac{3\sin^2 i\cos 2\theta}{8a^2}\right)\left[4\cos\theta + 5q_1 + 3\left(q_1\cos 2\theta + q_2\sin 2\theta\right)\right]$$

$$q_2{}^{sp2} = -\frac{3q_1\left(3-5\cos^2 i\right)}{8a^2}\sin 2\theta - \left(\frac{\sin^2 i}{8a^2}\right)\left(3\sin\theta - \sin 3\theta\right)$$
$$-\left(\frac{3\sin^2 i\cos 2\theta}{8a^2}\right)\left[4\sin\theta + 5q_2 + 3\left(q_1\sin 2\theta - q_2\cos 2\theta\right)\right]$$

$$\Omega^{sp2} = -\frac{\cos i}{4a^2}\left[3\sin 2\theta + 3\left(q_1\sin\theta + q_2\cos\theta\right) + \left(q_1\sin 3\theta - q_2\cos 3\theta\right)\right]$$

DISTRIBUTION LIST

DTIC/OCP
8725 John J. Kingman Rd, Suite 0944
Ft Belvoir, VA 22060-6218 1 cy

AFRL/RVIL
Kirtland AFB, NM 87117-5776 2 cys

Official Record Copy
AFRL/RVES/THOMAS ALAN LOVELL 1 cy